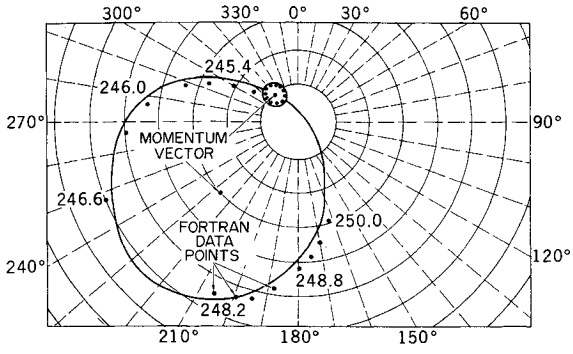

Fig. 6 Comparison of graphic method (with solid lines) showing coning and FORTRAN corroboration (dots).

The value of θ varied from maximum to minimum in precisely the same time periods. The spin of the vehicle was measured using the α signal during early and late flight and was found to be a constant 9.09 cps. The α signals more precisely define the spin time than the lateral θ signals. The total angular momentum of the vehicle is divided between the spin and cone periods, and a change in one means a change in the other, for a constant mass in space. From 70 sec to 245 sec, the variation in α is sinusoidal. A phase relationship with the maximum and minimum θ's was established, and, by plotting these positions, it was found that the vehicle coned six times about a momentum vector of altitude 80° and azimuth 320°. The cone angle was 6.5° and the period was 32.72 sec.

From 20 to 95 sec, the change in latitude and longitude indicated, through the radar plots, the velocity vector. The velocity vector during the powered portion of the flight is the average attitude of the vehicle. From this portion of the flight, the phase angle between the sun and magnetic south point was checked. This confirms the placement of the α sensors and the magnetometers within the payload.

At 244.75 sec (Fig. 6) the second stage separated from the payload and α began to vary sinusoidally from 27° to 94°. The period of the new large cone was found to be 6.25 sec, and the coning angle was $\backsim$67° about a new momentum vector. The new momentum vector's altitude was 60°, and its azimuth was 229°. It coned 10 times about this new vector before re-entry into the atmosphere.

At 259 sec, 51 solar signals were counted on the telemetry record, as were 50 magnetic aspect maximum signals on the lateral magnetometer. It was noted that the former coincided with the latter. One magnetometer maximum signal was lost because the vehicle coned once around the magnetic south point in the same interval. In the manner of Fig. 4, positions were plotted for the solar and magnetic aspect angles for both early and late flight (Fig. 6). The two skewed ellipses in Fig. 6 represent the epicycloidal motion immediately before and after ejection of the second stage and the consequent change in the momentum vector.

In Fig. 5, the 45° transparency (corresponding to the rocket's altitude) has been placed with its center directly over the nose position at 246 sec after liftoff. At this time, the rocket's altitude is about 45° and the azimuth is 276°. The rest of the sky, seen from the rocket nose, was then mapped by this transparency, and the aspect angle at the vehicle and the azimuth and altitude of any other celestial body can be plotted.

Figure 6 also compares the values from the FORTRAN analysis and data from the graphic analysis. Agreement is within 2°.

Reference

[1] Miller, C. F., Jr., "A Graphic Method for Determining the Absolute Attitude of Sounding Rocket Vehicles," TN D-5172, May 1969, NASA.

Heat Conduction through Fins with Nonadiabatic Tips

Y. S. Lou*
University of Delaware, Newark, Del.

Nomenclature

h = convective film coefficient
k = thermal conductivity
L = length of longitudinal fin
L_c = corrected length of a longitudinal fin
N = $(hp/ks)^{1/2}$
p = surface area per unit width of fin
q = heat flux
r = radius
r_{2c} = corrected outer radius of a radial fin
s = cross-sectional area per unit width of fin
T, T_f = temperature, and temperature of ambient fluid
δ = half-thickness of fin
ϵ = length of extended tip
θ = $T - T_f$
I_0, K_0 = zeroth-order modified Bessel functions of the first and second kinds

Introduction

FINS are commonly used in many heat exchanger applications. Fin geometries are diverse and are selected on the basis of efficient performance, minimum weight, and ease of manufacture. For those cases where the heat transfer from the fin tip is negligible, the adiabatic boundary condition facilitates obtaining exact solutions. However, in many cases the fin tip is not adiabatic, yielding a boundary condition quite involved for all but simple fin geometries. Harper and Brown[1] proposed an approximation technique for such cases, in which an imaginary extension is added to the fin tip. The temperature of the extension is assumed constant, and the heat flow from the end of the actual fin is dissipated through the two sides of the extension, such that the end of the imaginary tip is adiabatic. They approximate the length ϵ of the extension as one-half the actual thickness of the fin. When compared to the exact solution, this approximation is not accurate for certain combinations of fin geometry and operating conditions.[2]

This Note presents a method for *calculating* the length ϵ by treating the imaginary extension as a fin with an adiabatic tip, such that the heat flow at the base of the extension equals the heat loss from the tip of the actual fin. In this manner, variable temperature is allowed in the extension, and ϵ can be calculated directly. Theoretically, the new method should lead to exact solutions for predicting the heat conduction rate. We shall illustrate the method for both longitudinal and radial fins of constant thickness. For simplicity, the following assumptions shall be made in both cases: steady-state operation, uniform thermal conductivity (k = const), uniform convective film coefficient (h = const), one-dimensional temperature distribution, i.e., $k/h\delta \gg 1$, and uniform fluid temperature (T_f = const).

Description of the Problem

Case A: Longitudinal fin of constant thickness

Consider a fin of length L and thickness 2δ used to transfer heat from a body at uniform temperature T_0 (Fig. 1). Taking a small element Δx, a heat balance in the x direction is

$$sk\frac{\partial T}{\partial x} - \left[sk\frac{\partial T}{\partial x} + \frac{\partial}{\partial x}\left(ks\frac{\partial T}{\partial x}\right)\Delta x\right] - hp(T - T_f)\Delta x = 0 \quad (1)$$

Received May 21, 1969.
* Assistant Professor, Department of Mechanical and Aerospace Engineering. Member AIAA.

From the preceding assumptions, and letting $\theta \equiv T - T_f$ and $N \equiv (hp/ks)^{1/2}$, Eq. (1) can be reduced to

$$d^2\theta/dx^2 = N^2\theta \tag{2}$$

The general solution of Eq. (2) is

$$\theta = C_1e^{Nx} + C_2e^{-Nx} \tag{3}$$

For a fin with adiabatic tip, the boundary conditions are $\theta_{x=0} = \theta_0$ and $(d\theta/dx)_{x=L} = 0$. The solution of Eq. (3) for these conditions is

$$\theta/\theta_0 = \cosh[N(L - x)]/\cosh(NL) \tag{4}$$

and the heat flow at the root is

$$q_{x=0} = skN\theta_0 \tanh(NL) \tag{5}$$

For a fin with nonadiabatic tip, the second boundary conditions now becomes $-ks(d\theta/dx)_{x=L} = hs\theta$.

Although the exact solution of Eq. (3) with the latter boundary condition and $\theta_{x=L} = 0$ is easy to obtain for this case, the following is presented to illustrate the proposed method and how it can be applied to the case of more complex geometries for which the exact solutions are unwieldly.

In the Harper and Brown[1] approximation, the temperature of the extended portion was assumed to be uniform. Equating the heat loss from the surface to the heat loss at the fin tip, $sh\theta_L = 2h\theta_L\epsilon$, their length for the fin extension was (for unit width) $\epsilon = s/2 = \delta$, and the corrected length of the fin was $L_c = L + \epsilon = L + \delta$. The heat flow at the base of the actual fin was then *approximated* by substituting L_c for L in Eq. (5).

If, instead, we treat ϵ the imaginary extension as a new fin, such that the heat loss from the actual fin tip is the heat conducted into the base of the extension, and the tip of the extension is adiabatic, the heat balance becomes

$$sh\theta_L = skN\theta_L \tanh(N\epsilon)$$

which gives

$$L_c = L + \epsilon = L + (1/N) \tanh^{-1}(h/kN) \tag{6}$$

We substitute this L_c for L in Eq. (5) and reduce the result to the following form by using trigometric relationships:

$$q_{x=0} = skN\theta_0 \frac{\sinh(NL) + (h/kN)\cosh(NL)}{\cosh(NL) + (h/kN)\sinh(NL)} \tag{7}$$

Since Eq. (7) is the exact solution for the case of a longitudinal fin with nonadiabatic tip,[2] we have shown that the exact solution can be obtained with the improved method.

Case B: Radial fin of constant thickness

For a radial fin of inner radius r_1, outer radius r_2, and thickness 2δ (Fig. 2), the heat balance for a small radial element of length dr can be written as

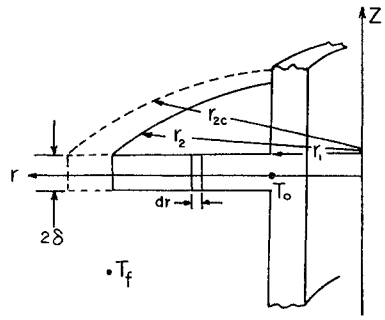

Fig. 2 Denotation for radial fin of constant thickness.

$$ks\frac{1}{r}\frac{\partial}{\partial r}\left(r\frac{\partial\theta}{\partial r}\right) - hp\theta = 0 \tag{8}$$

or

$$r^2\frac{\partial^2\theta}{\partial r^2} + r\frac{\partial\theta}{\partial r} - N^2r^2\theta = 0 \tag{9}$$

The solution to this equation is given in terms of modified Bessel functions as

$$\theta = C_1I_0(Nr) + C_2K_0(Nr) \tag{10}$$

If the fin tip is insulated and the temperature at the base θ_0 is given, the boundary conditions are

$$\theta_{r=r1} = \theta_0, \ (d\theta/dr)_r = r_2 = 0 \tag{11}$$

Differentiating and substituting Eq. (10) into Eq. (11) and solving for the constants C_1 and C_2 yields the following relation for temperature distribution:

$$\frac{\theta}{\theta_0} = \frac{I_0(Nr)K_1(Nr_2) + I_1(Nr_2)K_0(Nr)}{I_0(Nr_1)K_1(Nr_2) + I_1(Nr_2)K_0(Nr_1)} \tag{12}$$

The heat flow at the base is then calculated by

$$q_{r=r1} = -4\pi r_1k\delta\theta_0N \times \frac{+K_1(Nr_2)I_1(Nr_1) - I_1(Nr_2)K_1(Nr_1)}{I_0(Nr_1)K_1(Nr_2) + I_1(Nr_2)\ K_0(Nr_1)} \tag{13}$$

If the fin is not insulated at the tip, the second of Eqs. (11) becomes

$$(d\theta/dr)_{r=r_2} = -(h/k)\theta_L \tag{14}$$

The solutions for this case[3] are quite involved:

$$\frac{\theta}{\theta_0} = \frac{I_0(Nr) + \gamma K_0(Nr)}{I_0(Nr_1) + \gamma K_0(Nr_1)} \tag{15}$$

$$q_{r1} = -4\pi r_1k\delta\theta_0N\left\{\frac{I_1(Nr_1) - \gamma K_1(Nr_1)}{I_0(Nr_1) + \gamma K_0(Nr_1)}\right\} \tag{16}$$

where

$$\gamma = \frac{(h/kN)I_0(Nr_2) + I_1(Nr_2)}{K_1(Nr_2) - (h/Nk)K_0(Nr_2)}$$

The Harper and Brown technique[1] for a fin of this geometry yields a simple solution when the temperature of the imaginary extension is assumed uniformly equal to θ_L. A heat balance around the extension gives

$$q_{r2c} = 4\pi r_2\delta h\theta_L = 2\pi(r_{2c}^2 - r_2^2)h\theta_L \tag{17}$$

where r_{2c} is the corrected length of the radial fin; or r_{2c} is the corrected length of the radial fin; or $r_{2c} = r_2(1 + 2\delta/r_2)^{1/2}$, and for $\delta \ll r_2$

$$r_{2c} = r_2 + \epsilon = r_2 + \delta \tag{18}$$

This r_{2c} is then substituted for r_2 in (13).

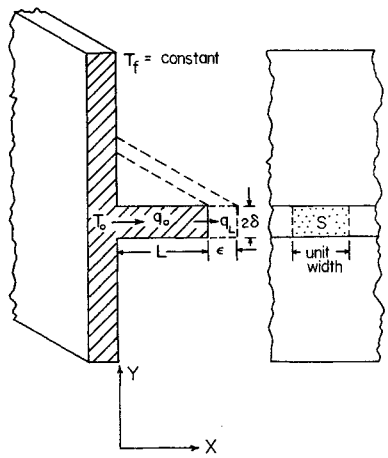

Fig. 1 Denotation for longitudinal fin of constant thickness.

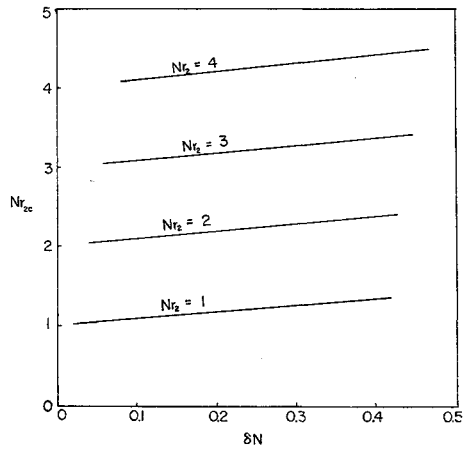

Fig. 3 Graphical solution for Eq. (21).

In the improved method, we imagine the fin extended to r_{2c} such that the temperature gradient will be zero at $r = r_{2c}$. The heat flow at $r = r_2$ is

$$q_{r=r_2} = 4\pi r_2 \delta h \theta_L \tag{19}$$

This quantity of heat must be dissipated through the two surfaces of the extended fin which is given in Eq. (13) by replacing r_1, r_2, and θ_0 with r_2, r_{2c}, and θ_L, respectively. Equating the result to the right side of Eq. (19), we obtain

$$-\delta N = \frac{I_1(Nr_2)K_1(Nr_{2c}) - I(Nr_{2c})K_1(Nr_2)}{I_0(Nr_2)K_1(Nr_{2c}) + I_1(Nr_{2c})K_0(Nr_2)} \tag{20}$$

We now have an equation with one unknown, r_{2c}, which can be arranged to yield

$$\frac{I_1(Nr_{2c})}{K_1(Nr_{2c})} = \frac{I_1(Nr_2) + \delta N I_0(Nr_2)}{K_1(Nr_2) - \delta N K_0(Nr_2)} \tag{21}$$

with the right side containing functions of known parameters. Equation (21) cannot be solved analytically for r_{2c}, since r_{2c} is the argument of the modified Bessel functions. It can be solved, however, by method of iteration to any accuracy desired. A graphical solution of the Eq. (21) is given in Fig. 3. Knowing the values of r_2 and δ, the corresponding value of r_{2c} can be read from the graph. The heat transfer at the root, $q_{r=r_1}$ of a nonadiabatic radial fin is then obtained by replacing r_2 in Eq. (13) by this value of r_{2c}. Theoretically, the value of $q_{r=r_1}$ thus obtained should be identical to that obtained from the exact solution given in Eq. (16).

Concluding Remarks

This new method for treating the problem of heat conduction through finned surfaces is similar to the approximation method of Harper and Brown,[1] except that the length of the imaginary extended tip is calculated rather than being assumed, and no assumption of uniform temperature of the extended tip is used. Therefore, theoretically, it should lead to exact solutions of the heat conduction through finned surfaces with nonadiabatic tips. The only prerequisite for this method (as for the method of Ref. 1) is the existence of the solution for the case of the finned surface with an adiabatic tip, which is always much easier to obtain.

For the case of a longitudinal fin, an exact solution is obtained, because the simple fin geometry enables us to derive an explicit expression for the imaginary extension length ϵ. For the case of a radial fin, solutions are given in graphical form, because ϵ is part of the arguments of some modified Bessel functions. One may derive an approximate expression for ϵ by expending those Bessel functions into polynomials. However, the results of heat conduction obtained by retaining terms up to ϵ^2 are found[4] to be not much better than those calculated by the method of Harper and Brown.

References

[1] Harper, W. B. and Brown, D. R., "Mathematical Equations for Heat Conduction in the Fins of Air Cooled Engines," Rept. 158, 1922, NACA.

[2] Schneider, P. J., *Conduction Heat Transfer*, 2nd ed., Addison-Wesley, Reading, Mass., 1957, p. 63.

[3] Kraus, N. W., *Extended Surfaces*, Spartan, Baltimore, 1964.

[4] Woods, J. J., "An Improved Approximation Method for Predicting the Steady-State Performance of Extended Surfaces with Non-Adiabatic Tips," M.S. thesis, June 1968, Univ. of Delaware.

A New Concept for Low-Range Pressure Measurements on Full-Scale Flight Re-Entry Vehicles

J. M. Cassanto* and F. C. George†
General Electric Company, King of Prussia, Pa.

Introduction

LOW-RANGE pressure sensors are needed on re-entry test vehicles for base pressure measurements to determine the altitude of onset of boundary-layer transition. Absolute pressure transducers for this purpose tend to be large and bulky because they utilize an evacuated, hermetically sealed reference chamber. Since some leakage occurs even with the best hermetic seals, the reference chamber is made rather large to insure calibration stability and a long shelf life. The new concept[1] described herein avoids these problems by using a differential pressure sensor with a controlled leak rate (time constant) that vents to the vacuum of free space and uses the resultant vacuum as a reference pressure during reentry. The time constant can be made short for normal ballistic reentry trajectories or extremely long for planetary entry probe missions, thus insuring an accurate, reliable vacuum reference during entry. A vent tube restrictor/feedback loop containing a porous slug of metal with a known leak rate (Fig. 1) produces the time constant.

The concept of a differential pressure transducer with a time constant to measure absolute pressures has been used for years in wind tunnels and shock tunnels[2–4] but the proposed use on flight vehicles is new. In shock-tunnel tests, the differential sensor equalizes to the vacuum conditions in the test section prior to the test. During a short blowdown run, the calibration side of the transducer holds the vacuum long enough to sense the difference between the measured pressure and the vacuum. For the flight application, the time constant is designed so that the vacuum on the references side holds long enough ($t \sim 10$ sec.) to make the flight measurement. The flight prototype unit described herein (Fig. 2) employs a shock-tunnel-type (capacitance) transducer, has a range from 0 to 0.2 psid, weighs 6 oz, and has a volume of 6 in.[3] A comparable "off-the-shelf" absolute pressure sensor of equivalent range weighs 9 oz and has a volume of 9 in.[3]

Powered Flight and Re-Entry Pressure Simulation

For a typical short-duration ballistic flight ($\sim$340 sec), atmospheric pressure exists on each side of the diaphragm

Received May 6, 1969; revision received July 7, 1969.

* Supervising Engineer, Re-Entry Systems Operation, Aerodynamics Laboratory. Member AIAA.

† Specialist, Re-Entry Systems Operation, Aerodynamics Laboratory.